Directional distribution of acoustic energy density incident to a surface under reverberant condition

Cheol-Ho Jeong[a] and Jeong-Guon Ih[b]

[a]Acoustic Technology, DTU Elektro, Technical University of Denmark, Building 352, Ørsted plads, DK-2800 Kgs. Lyngby, Denmark
[b]KAIST, Dept. of Mechanical Engineering, Science Town, 305-701 Daejeon, Republic of Korea
chj@oersted.dtu.dk

Most acoustic measurements are based on the assumption of ideal conditions. One such ideal condition is a diffuse and reverberant field. In practice, a diffuse sound field cannot be achieved in a reverberation chamber. Particularly, the directional diffusion, which means the uniform angular distribution of incident energy onto surfaces, cannot be satisfied. Angle dependence of incident energy density was simulated by the phased beam tracing method by changing room shapes and source positions. It was found that acoustic energy density decreases with the angle of incidence. The shape of the averaged angular distribution is similar to the Gaussian distribution. Long distance between the source and the target surface highlights the normally incident components. To get a fairly uniform distribution, the acoustic centre of the source should be close to and aligned with the periphery of the absorption sample.

1   Introduction

The diffuse field is an idealized concept and the underlying principle of standardized measurements and theoretical derivations. For a perfectly diffuse field, two assumptions must be satisfied [1]:

1. The local energy density in a room is uniform (the spatial diffusion),

2. The energy is uniformly incident onto a surface from all directions (the directional diffusion).

The first assumption of the spatially uniform sound field cannot be satisfied near the boundaries, e.g., surfaces, edges, and corners. The interference of sound waves increases the acoustic energy near boundaries. At locations about one wavelength apart from boundaries, the deviation of sound pressure is bounded within 1 dB in a large reverberation chamber [2].

In spite of endeavours to obtain a diffuse sound field in a reverberation room, the second assumption of the random incidence is very hard to fulfil. Especially when a test specimen covers one surface such as absorption and sound transmission loss (STL) measurements, an ideal diffusivity is rarely obtained. In the calculation of STL, truncation of the angle of incidence was introduced as a compensation and typical values of the limiting angle vary from 70° to 85° based on empirical data [3,4]. This implies that acoustic energies are not uniformly incident on a sample surface. From this fact, one can imagine that grazingly incident energies are smaller enough to be neglected than other components.

The random incidence absorption coefficient is based on the fact that intensities of the incident sound are uniformly distributed over all possible directions. These assumptions result in Paris formula associated with $\sin(2\theta)$ [5]. However, the random incident coefficient from measured impedance data shows a noticeable discrepancy with the measured absorption coefficient by Sabine's formula (sometimes referred to as Sabine absorption coefficient) [6]. Measured absorption coefficients are overestimated for small absorber samples and sometimes exceed unity, even for a nearly locally reacting surface. Reasons for higher measured absorption coefficients have been widely accepted to be the finiteness of samples and the edge diffraction [7-13].

To match the theoretical value with measured data, several works have been studied. Kang and Ih [14] applied the Gaussian weighting function for STL calculations and

excellent agreement with measured data was achieved. For the absorption measurement, Makita and Fujiwara took the initiative to examine the non-uniformity of sound energy [15], although they had no idea of the angular distribution of the incident energy distribution. The result revealed that the maximum value can exceed unity depending on the maximum value of directional distribution. Thomasson [16,17] concentrated on the size effect of an absorption sample, by introducing the concept of averaged radiation impedance. This approach also modifies the law of cosine for oblique incidence. The correction for the finite size enables absorption coefficients to exceed unity. In the meantime, several semi-empirical corrections were suggested. London defined a quantity called equivalent real impedance and used this quantity for computing the reverberation absorption coefficient [13]. This study aims to investigate the angular distribution of incident sound onto an absorber sample in a reverberant sound field by means of the phased beam tracing method. The simulation results can be used as a weighting function in calculating the angle-weighted absorption coefficient.

2   Angular weighting function

The phased beam tracing method (PBTM) was employed in order to simulate the angular distribution of the reverberant energy density. The phased beam tracing method is a modified version of the triangular beam tracing method (for example, [18]) by retaining phase information during the beam propagation [19,20]. Triangular beams, which are emitted from a source, are followed by their central axes without splitting algorithm. Only specular reflection is adopted during the tracing and negligible absorption coefficient of 0.01 is assigned for all surfaces irrespective of frequency. Results of this geometrical acoustics technique are particularly advantageous by providing the information on the incidence angles and energies at those times.

Two chambers were chosen as test examples: one is a rectangular parallelepiped chamber and the other is a room with non-parallel surfaces. In accordance with ISO 354 [21] and ASTM C 423-02 [22], sources are located at trihedral corners of the rooms. It is assumed that an absorber sample covers one whole surface of the rooms. Therefore, one can collect the information of beams incident onto that specific surface. This surface, on which the absorber is installed, is named as the target surface.

During the beam tracing, the information on the directional energies and angles of incidence is saved. Acoustic energy decays inversely proportional to r^2 and it is reduced by $(1-\alpha_i)$ whenever beam hits surfaces. Here, r denotes the travelling distance and α_i the absorption coefficient of ith

surface. For a steady-state condition, a total directional energy from θ_i is calculated by summing all components over the interval, $[\theta_{i,l} \; \theta_{i,u}]$. Here, $\theta_{i,l}$ and $\theta_{i,u}$ are lower limit and upper limit of the interval, respectively and θ_i is the arithmetic mean of those values. The directional energy density is the ratio between the total incident sound energy, E_θ, and the corresponding solid angle, Ω_θ. Using the generalized concept of solid angle in terms of spherical polar coordinate, θ and φ, respectively (Fig.1), the solid angle element is expressed as $d\Omega = \sin\theta d\theta d\varphi$. By integrating the azimuth angle, φ, from zero to 2π and the polar angle, θ, over the corresponding interval of $[\theta_{i,l} \; \theta_{i,u}]$, one can find the solid angle at θ_i, as follows:
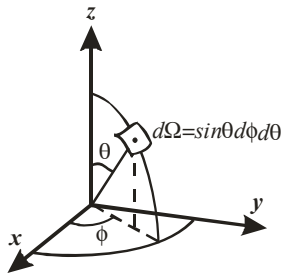

Fig. 1. Spherical polar coordinate representing solid angle.

$$\Omega_{\theta_i} = \int_0^{2\pi} \int_{\theta_{i,l}}^{\theta_{i,u}} d\Omega = 2\pi \int_{\theta_{i,l}}^{\theta_{i,u}} \sin\theta \, d\theta . \tag{1}$$

The solid angle increases with angle of incidence. The directional energy density is defined as the total directional energy incident from θ_i divided by the corresponding solid angle as follows:

$$D(\theta_i) = \frac{E_{\theta_i}}{\Omega_{\theta_i}} . \tag{2}$$

3 A rectangular shaped room

Lecture rooms and reverberation chambers are generally rectangular shaped. This kind of room usually has a problem that the interference is strong due to pairs of parallel surfaces. In this study, all surfaces are assumed smooth and scattering is not taken into account.

The test rectangular room model is shown in Fig. 2(a). The edge lengths are 6.2 m × 5.1 m × 3.0 m and the volume is 94.8 m³. The surface of interest is parallel to the y-z plane being 6.2 m apart from the y-z plane, say (6.2, y, z). A sample specimen for absorption measurement is supposed to cover the whole surface. To examine the effect of source locations, three source locations were chosen. One is situated very close to the centre of the surface of interest. The others are located near trihedral corners of the rectangular room in accordance with the standards.

The first omni-directional source is located at (6 m, 2 m, 1.5 m). In the simulation, 8000 beams are emitted from the source. It is obvious that directly transmitted energies from the source to the target surface contribute the most to total energies. In Fig. 2(a), directly transmitted central axes of triangular beams (hereafter direct ray) that strike the target surface were depicted. Among 8000 emitted beams, 3537 beams strike the sample surface, because the source is very close to the surface and located off the central position of the surface. In Fig. 2(b), the number of detected rays at the target surface is shown with intervals of 10°. The detected

number of direct rays increases with an angle of incidence in this case. Figure 2(c) shows a contour plot of the incidence angle of direct rays onto an absorption sample by steps of 10°. Apparently, the equal-angle contours become concentric circles. Radii of concentric circles get exponentially larger. It means solid angle increases with increasing angle of incidence. The normally incident sound is confined to a very limited area, while grazing incidence occupies the largest area. In Fig. 2(d), the directional energy density of direct rays is shown, with intervals of 15°. The general trend of the direct energy density is to decrease with angle of incidence. It should be noted here that Fig. 1 shows the results by direct propagation.

In Fig. 3, one can find the angular distribution of reverberant acoustic energy density by accounting 35 successive reflections. The overall trend of reverberant energy density is similar to that of direct sound, because the directly transmitted energy overwhelms the total sound field. This normalized energy density shows a similarity with the result by Kang and Ih [14].
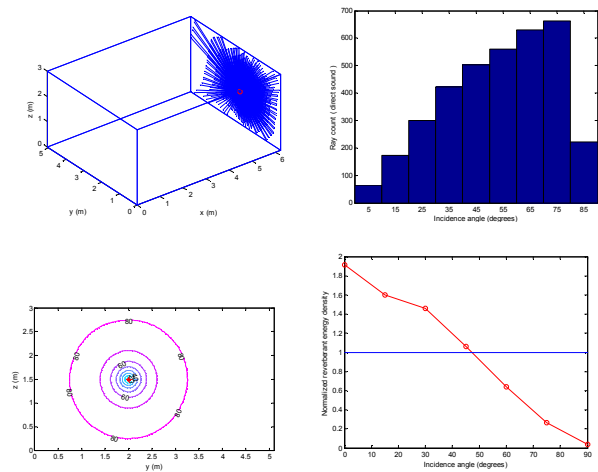

Fig. 2. Simulation results for direct acoustic energy. (a) Room model, (b) the ray count, (c) the equal incidence angle contour, (d) the direct acoustic energy density.
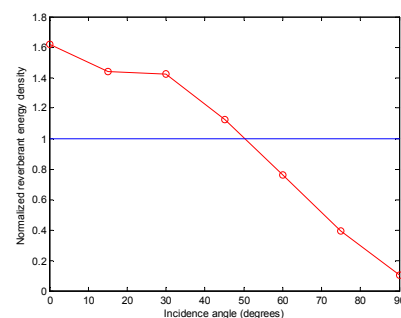

Fig. 3. Acoustic energy densities for reverberant field.

There are only two trihedral corners due to the symmetry of the room. In Fig. 4, the simulation results are shown when a source is located at (6 m, 0.2 m, 0.1 m), close to the surface of interest. The reverberant energy density shows a good similarity with that of the previous case.

In Fig. 5, source location is moved to another trihedral corner, which is far from the surface of interest, and situated at (0.2 m, 0.2 m, 0.2 m). The normally incident reverberant acoustic density (see Fig. 5(b)) is 18% higher

than the previous case, due to lack of obliquely incident direct rays. (No direct rays above 42° can reach the target surface)
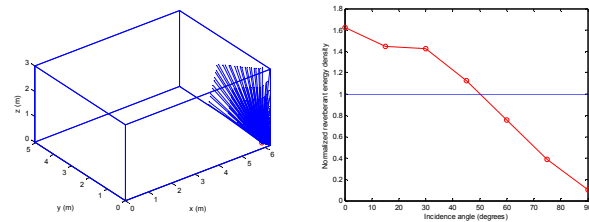

Fig. 4. The room model and the reverberant acoustic energy density for the source at (6 m, 0.2 m, 0.1 m).
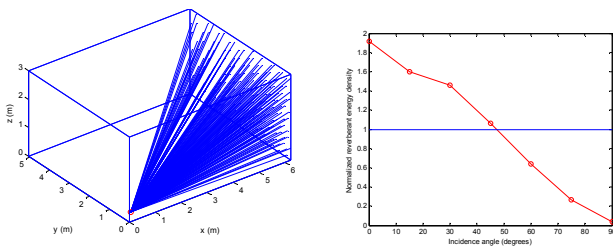

Fig. 5. The room model and the reverberant acoustic energy density for the source at (0.2 m, 0.2 m, 0.2 m).

For equally-spaced 90 (6×5×3) source locations, angular distributions of reverberant energy density are simulated and averaged. Source locations are determined by combining x values of (1, 2, 3, 4, 5, 6 m) and y values of (1, 2, 3, 4, 5 m) and z values of (0.2, 1.1, 2 m). In Fig. 6(b), the normalized and averaged distribution is shown. The averaged reverberant energy density clearly shows that oblique incidence over 70° contributes little to the total energy density.
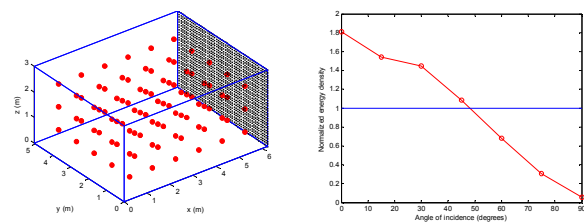

Fig. 6. 90 equally-spaced sources and the averaged reverberant energy density.

4   A room with non-parallel walls

In Fig. 7(a), a reverberation room with non-parallel surfaces was taken as an example. The volume of the space is 179 m^3 and absorption coefficient is also 0.01, irrespective of surface and frequency. Geometrical nodal points of this model are listed in Table 1. The target surface was *x-z* plane. Simulation was carried out for five trihedral corner sources in this room. Figure 7 shows the result when the source is located at (-1.5 m, 3.5 m, 0.2 m). Due to the geometry of room and the source location, direct ray cannot arrive from the normal direction. Both Figs. 7(b) and 7(c) show that there is the lower limiting angle of 23°. Direct energy density shows a single peak at 45°. In contrast, the reverberant energy density has two peaks at 0 and 43°. This

result is apparently different from the previous result which shows a decreasing tendency with angle of incidence. Energy is re-distributed due to the lack of direct normal incident rays.
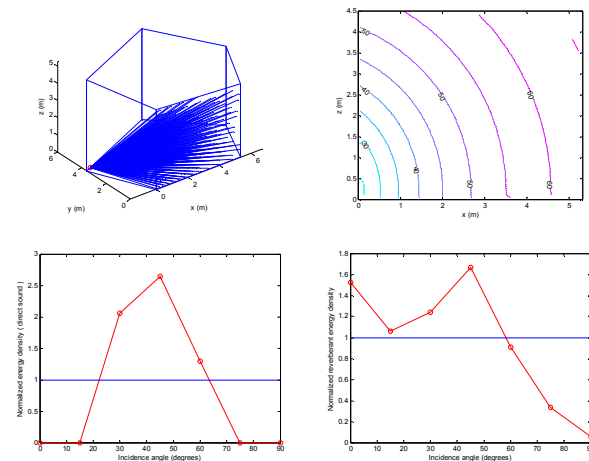

Fig. 7. Simulation results for direct acoustic energy. (a) Room model, (b) The equal incidence angle contour, (c) the direct acoustic energy density, (c) the reverberant acoustic energy density.

Coordinate Node numbering	x	y	z
1	0	0	0
2	5.32	0	0
3	6.71	2.99	0
4	3.72	6.02	0
5	-1.63	3.61	0
6	0	0	4.66
7	5.32	0	4.30
8	6.71	2.99	4.62
9	3.72	6.02	5.30
10	-1.63	3.61	5.30

Table 1. Geometrical node data of a reverberation chamber.

In Fig. 8, the source is located at the farthest distance of all sources. As discussed in the previous chapter, a long distance between a source and a target surface emphasizes the importance of normally incident energy. For the reverberant energy density, an abrupt decrease was found above 45° and the contribution becomes less than 0.5.
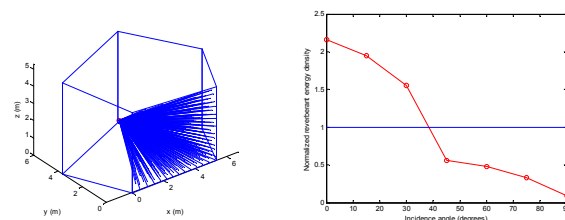

Fig. 8. The room model and the reverberant acoustic energy density for the source at (3.7 m, 5.9 m, 0.2 m).

For the source at (6.6 m, 2.9 m. 0.2 m), the results in Fig. 9 show a strong similarity with the results in Fig. 7. As the sound source is invisible from the normal direction of the target surface, the incidence angle of 45° becomes pronounced. The double peak shaped distribution was

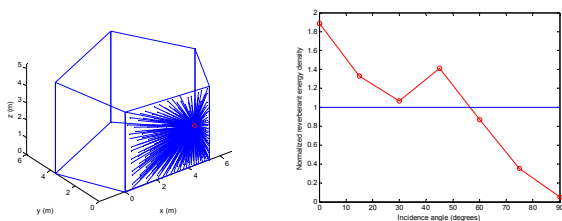found for the reverberant acoustic energy density in Fig. 9(b).

Fig. 9. The room model and the reverberant acoustic energy density for the source at (6.6 m, 2.9 m. 0.2 m).

The remaining two source locations at (5.3 m, 0.2 m, 0.2 m) and (0 m, 0.2 m, 0.2 m) are closer to the target surface. The reverberant acoustic energy densities of two cases show a large difference: one continuously decrease in Fig. 10(b), while the other is relatively uniform until 60° in Fig. 11(b).
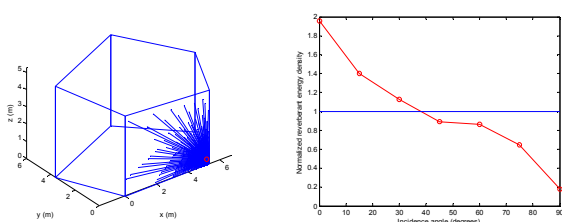

Fig. 10. The room model and the reverberant acoustic energy density for the source at (5.3 m, 0.2 m, 0.2 m).
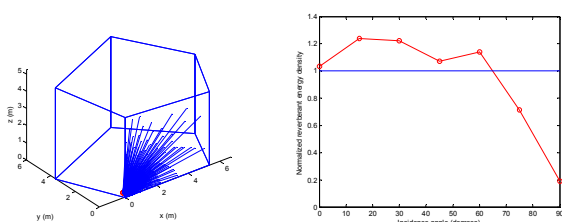

Fig. 11. The room model and the reverberant acoustic energy density for the source at (0 m, 0.2 m, 0.2 m).

The discrepancy originates from the fact that the source for Fig. 10 is misaligned inwardly from the periphery of the target surface, as shown in Fig. 12. If a source is located inside the periphery of the target surface (x coordinate varies from 0 to 5.32 m), then normally incident energy is too much distinguished. Therefore one fails to have the uniform distribution. The result in Fig. 13, which shows the effects of source locations, supports the above statement. By changing x-coordinate of a sound source position from 5.3 m to 5.33 m with steps of 0.005 m, one can clearly see that the normal energy density is accentuated, when the source is located inside the fringe of surface (refer to the symbols ○ and △). When a source moves away from the fringe, a normally incident energy gets weakened owing to the absence of direct normal components (symbols ▷ and ◁). In order to have a relatively uniform energy distribution, it is desirable to locate the acoustic centre of sound source perpendicularly off the periphery of the surface. A slight misalign might seems acceptable because of the limited spatial resolution of the geometrical acoustics method.
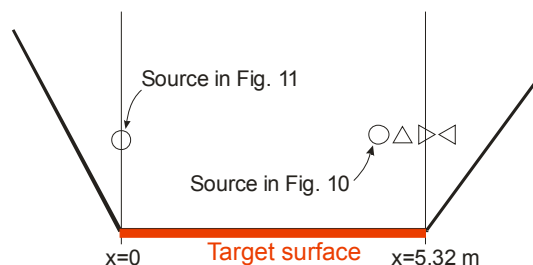

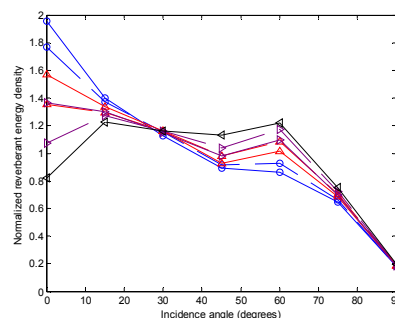Fig. 12. Location of sources in Figs. 10 and 11.

Fig. 13. A comparison of reverberant energy density. x-coordinate of sources varies from 5.30 m to 5.33 m with a step of 0.05 m. ─○─ , x=5.300 m; ─○─ , x=5.305 m; ─△─ , x=5.310 m; ─△─ , x=5.315 m; ─▷─ , x=5.320 m; ─▷─ , x=5.325 m; ─◁─ , x=5.330 m (see Fig. 12).

In Fig. 14, the effect of a distance between a source and the target surface is shown. Provided that the x-coordinate of source locations is fixed to 5.32 m (perpendicularly off the periphery), distances from the surface to a source were changed to 0.01 m, 0.2 m, 0.5 m, 1 m. The shorter the distance, the more uniform the reverberant acoustic energy is. It can be concluded that the preferable source location for the uniform reverberant energy is the possibly closest peripheral corner position. For a rectangular shaped room, this ideal position does not exist, because all possible source locations are found inward the periphery.
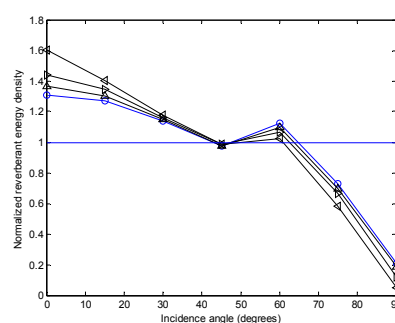

Fig. 14. Effects of distance on the reverberant energy density. ─○─ , d=0.01 m; ─△─ , d=0.20 m; ─▷─ , d=0.50 m; ─◁─ , d=1.00 m. x-coordinate of sources is set to 5. 32 m.

In Fig. 15, the averaged result over 96 equi-spaced source locations is shown. The averaged result shows an acceptable correspondence with the result of the rectangular room (Fig. 6), but differs from the result by the five corner sources (tick line). The calculated reverberant energy densities will be used as a weighting factor in computing absorption coefficients from surface impedances.
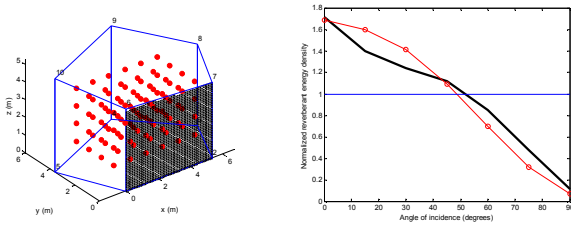
Fig. 15. 96 equally spaced sources and the averaged reverberant energy density. Solid line shows the averaged value over 5 corner sources.

5   Conclusion

The angular distribution of incident energy density has been simulated for the rectangular room and the reverberation chamber with non-parallel surfaces by using the phased beam tracing method. Depending on the source position, a large variation was found. Generally the acoustic energy decreases with increasing angle of incidence. To achieve a uniform distribution, the source should be located perpendicularly off the periphery of the target surface, as close as possible to the target surface. Therefore a room with non-parallel walls is advantageous for obtaining a uniform distribution. Long distance from a source to a target surface results in the concentration of acoustic energy near normal direction.

Acknowledgments

References

[1] T. J. Schultz, "Diffusion in Reverberation rooms," Journal of Sound and Vibration 16, 17-28 (1971).

[2] R. V. Waterhouse, "Patterns in reverberant sound fields," Journal of the Acoustical Society of America 27, 247-258 (1955).

[3] L. L. Beranek, Noise reduction (New York, McGraw-Hill), 1971, chapter 13.

[4] R. E. Jones, "Inter-comparisons of laboratory determinations of airborne sound transmission loss," Journal of the Acoustical Society of America 66, 148-164 (1950).

[5] E. T. Paris, "On the reflection of sound from a porous surface," Proceedings of Royal Society of London 115A, 407-419 (1927).

[6] D. Olynyk and T. D. Northwood, "Comparison of reverberation room and impedance tube absorption measurement," Journal of the Acoustical Society of America 36, 2171-2174 (1964).

[7] E. D. Bruijn, "The edge effect of sound absorbing materials," Proceedings of International Congress on Acoustics H35 (1965).

[8] T. T. Wolde, "Measurements on the Edge-Effect in Reverberation Rooms," Acustica 18, 207-212 (1967).

[9] W. Kuhl, "Der Einfluss der Kanten auf die Schall-absorption poroser Materilien," Acustica 10, 264 (1960).

[10] T. W. Bartel, "Effect of absorber geometry on apparent absorption coefficients as measured in a reverberation chabmer," Journal of the Acoustical Society of Ameria 69, 1065-1074 (1981).

[11] C. W. Kosten, "International comparison measurement in the reverberation room," Acustica 10, 400-411 (1960).

[12] P. E. Sabine, "Specific normal impedances and sound absorption coefficients of material," Journal of the Acoustical Society of Ameria 12, 317-322 (1941).

[13] A. London, "The determination of reverberant sound absorption coefficients from acoustic impedance measurements," Journal of the Acoustical Society of Ameria 22, 263-269 (1950).

[14] H.-J. Kang and J.-G. Ih, "Prediction of sound transmission loss through multilayered panels by using Gaussian distribution of directional incident energy," Journal of the Acoustical Society of America 107, 1413-1420 (2000).

[15] Y. Makita and K. Fujiwara, "Effects of Precision of a reverberant absorption coefficient of a plane absorber due to anisotropy of sound energy flow in a reverberation room," Acustica 39, (1978).

[16] S.-I. Thomasson, "On the absorption coefficient," Acustica 44, 265-273 (1980).

[17] S.-I. Thomasson, Theory and experiments on the sound absorption as function of the area. Report TRITA-TAK 8201, KTH (1982).

[18] T. Lewers, "A Combined Beam Tracing and Radiant Exchange Computer-Model of Room Acoustics," Applied Acoustics 38, 161~178 (1993).

[19] A. Wareing and M. Hodgson, "Beam-tracing model for predicting sound field in rooms with multilayer bounding surfaces," Journal of the Acoustical Society of America 118, 2321~2331 (2005).

[20] C.-H. Jeong, J.-G. Ih and J. H. Rindel, "An Approximate Treatment of Reflection Coefficient in the Phased Beam Tracing Method for the Simulation of Enclosed Sound Fields at Medium Frequencies," To appear in Applied Acoustics (2008).

[21] Anon., ISO 354: Acoustics - Measurement of sound absorption in a reverberation room (1985).

[22] Anon., ASME C 423-02: Standard test method for sound absorption and sound absorption coefficients by the reverberation room (2003).